Proc. Natl. Acad. Sci. USA
Vol. 91, pp. 11070–11074, November 1994
Cell Biology

Spatially controlled adhesion, spreading, and differentiation of endothelial cells on self-assembled molecular monolayers

(surface modification/photolithography/angiogenesis/fibronectin)

B. J. SPARGO*†, M. A. TESTOFF*, T. B. NIELSEN‡, D. A. STENGER*, J. J. HICKMAN§, AND A. S. RUDOLPH*

*Center for Biomolecular Science and Engineering, Code 6900, Naval Research Laboratory, Washington, DC 20735-5000; ‡Wound Repair Enhancement Program, Naval Medical Research Institute, Bethesda, MD 20889-5055; and §Science Applications International Corporation, McLean, VA 22102

Communicated by Judah Folkman, July 1, 1994

ABSTRACT **Chemically modified glass substrates were used to demonstrate differential adhesion, growth, and differentiation of endothelial cells. Endothelial cells were examined for adhesion and growth on glass, glass treated with *N*-(2-aminoethyl)-3-aminopropyl trimethoxysilane (EDA), or EDA with a subsequent treatment with physically adsorbed extracellular matrix components human fibronectin and heparin sulfate. EDA and EDA/human fibronectin showed similar abilities to support adhesion, spreading, and proliferation of endothelial cells. In contrast, heparin sulfate inhibited endothelial cell adhesion to EDA. Differentiation of endothelial cells resulting in precapillary cord formation was triggered by addition of basic fibroblast growth factor (bFGF). On EDA and EDA/human fibronectin bFGF causes confluent endothelial cell monolayers to differentiate and form cords, which resulted in a large-scale spatial redistribution of cells on the surface. Formation of organized neovascular assemblies was demonstrated on coplanar molecular patterns of EDA and a nonadhesive perfluorinated alkylsilane (tridecafluoro-1,1,2,2-tetrahydrooctyl)-1-dimethylchlorosilane (13F). Endothelial cells preferentially adhered to the EDA lines and after 24–48 hr, microfilaments aligned with the long axes of the patterned EDA region. Finally, endothelial cells that became confluent within the confines of the EDA region (bound by the nonadhesive, 13F domains) were observed to differentiate into neovascular cords in long-term culture (7–10 days) with bFGF.**

The formation of organized multicellular assemblies of endothelial cells into neovascular structures has been induced by a variety of soluble differentiation factors (1, 2). These multicellular assemblies depend on both cell–cell and cell–substrate interactions. This process, angiogenesis, has important implications in tumorigenesis (3–5) and vascular implant material development (6). The physical and chemical character of the surface has been implicated as a determinant of angiogenesis *in vitro*, with focus on the chemical and physical adsorption of extracellular matrix molecules (i.e., fibronectin, collagen, laminin, heparin sulfate, and hyaluronic acid). The modification of material surfaces to control adhesion, spreading, and growth of endothelial cells has important technological implications for improving compatibility of vascular materials.

The characteristics of the substrate surface that determine adhesion and spreading of cells have been examined for a variety of substrate types and chemical compositions (6). Treatment of culture plastics with extracellular matrix molecules such as laminin, collagen, and fibronectin, results in an increase in the number of cells that initially adhere and in the rate of proliferation, both of which depend on the matrix protein type (6, 7). However, the role of substrate surface in promoting angiogenesis is not well understood, although it is clearly a critical determinant in this process.

Several approaches have also demonstrated the potential for controlling the spatial distribution of cells on the surface. Carter (8, 9) and later Harris (10), using acetate-coated glass, created palladium islands and channels for studying single fibroblast cell reactions and clone formation. Kleinfeld and coworkers (11) fabricated high-resolution patterns of self-assembled monolayers (SAMs) of amino- and perfluoroalkylsilanes, which resulted in dissociated neurons that preferentially adhered to and developed electrically active associations within the geometrically defined regions. The use of SAMs to create regions of defined chemical reactivity also allows selective attachment of fibroblasts and endothelial cells to regions modified by covalently bound peptides that contain the Arg-Gly-Asp (RGD) binding domain (12–14).

In this study, a series of SAM-modified surfaces were examined for their ability to support adherence and facilitate growth and differentiation of endothelial cells. Patterned substrates, created by deep UV photolithography (15), were used to provide spatially defined regions that promoted adhesion, spreading of endothelial cells, and ultimately spatially defined neovascular assemblies on a two-dimensional surface.

MATERIALS AND METHODS

Reagents. Human fibronectin (hFN) was obtained from Collaborative Research. Heparin sulfate (HS) (≈7.5 kDa) was obtained from Sigma. *N*-(2-Aminoethyl)-3-aminopropyl trimethoxysilane (EDA) and (tridecafluoro-1,1,2,2-tetrahydrooctyl)-1-dimethylchlorosilane (13F) were used as procured from Hüls America (Bristol, PA).

Substrate Preparation. Patterned deposition of EDA and 13F was accomplished by using the photolithography method of Dulcey *et al.* (15). Glass substrates were washed in methanol/HCl, 1:1 (vol/vol) for 1 hr and 18 M H_2SO_4 for 1 hr followed by multiple washes with deionized water (18 MΩ). After the final wash, the substrates were immersed in boiling deionized water for 20 min, removed, and immersed in 1% EDA/94% (vol/vol) methanol/1 mM acetic acid/5% H_2O for 15 min. The substrates were then rinsed at least three times in anhydrous methanol and baked at 120°C for 5 min. 13F was deposited on either clean glass or patterned EDA surfaces by using a 1% (vol/vol) solution of the silane in anhydrous toluene for 1–3 hr, followed by at least four rinses in toluene, and baked 5 min at 120°C. EDA films were exposed to pulsed ArF excimer laser (193 nm) radiation (15 J/cm², 30 Hz) through a lithographic mask. Deep UV-irradiated regions of the substrate were resilanized with 13F

The publication costs of this article were defrayed in part by page charge payment. This article must therefore be hereby marked "*advertisement*" in accordance with 18 U.S.C. §1734 solely to indicate this fact.

Abbreviations: SAM, self-assembled monolayer; HUVE, human umbilical vein endothelial cell; EDA, *N*-(2-aminoethyl)-3-aminopropyl trimethoxysilane; 13F, (tridecafluoro-1,1,2,2-tetrahydrooctyl)-1-dimethylchlorosilane; bFGF, basic fibroblast growth factor; hFN, human fibronectin; HS, heparin sulfate; XPS, x-ray photoelectron spectroscopy; RGD, Arg-Gly-Asp.

†To whom reprint requests should be addressed.

as described above. Some substrates were further modified by the adsorption of hFN or HS. Substrates were incubated at 4°C in a sterile phosphate-buffered saline solution containing hFN (200 ng/ml) or HS (100 μg/ml) for 24 hr. Substrates were sterilized by using 70% (vol/vol) ethanol and rinsed in sterile phosphate-buffered saline before seeding with endothelial cells.

Substrate Characterization. The advancing water contact angle, $\theta_{a(H_2O)}$, of each substrate was measured by using the sessile drop method, as described (16). X-ray photoelectron spectroscopy (XPS) analysis was done to determine the extent of adsorption of hFN or HS to glass and EDA-treated glass. XPS spectra were obtained on a SSX-100 spectrometer (Surface Science Instruments) equipped with a concentric hemispherical analyzer. Spectra were referenced to the Si (2p3/2) peak at 102.4 eV (1 eV = $1{,}602 \times 10^{-19}$ J).

Cell Culture. Primary cultures of human umbilical vein endothelial (HUVE) cells were obtained from Clonetics (San Diego) and grown in culture medium M-199 containing 2% (vol/vol) fetal bovine serum, endothelial cell growth factor (10 ng/ml), hydrocortisone (1 μg/ml), and 0.4% (vol/vol) bovine brain extract at 37°C in 5% CO_2/air. HUVE cells were passed by using trypsin-EDTA between 50–80% confluency and were used between two and six passages. After growth to confluency on the substrates, the growth medium was replaced with medium M-199/basic fibroblast growth factor (bFGF) at 5 ng/ml/0.5% (vol/vol) fetal bovine serum. Primary cultures of porcine cerebral microvascular endothelial cells were initiated as described (17) and grown in medium M-199/10% (vol/vol) fetal bovine serum/heparin (100 μg/ml)/0.8% (vol/vol) retinal extract. The media were replaced every other day.

RESULTS

Substrate Characterization. The substrate surfaces were characterized by water contact angle measurements and XPS. Contact angle measurements determine the degree of hydrophobicity of a surface, and the values are inversely proportional to the surface free energy. Previous work (18) has shown that EDA forms highly ordered, reaction-site-limited monolayers with a $\theta_{a(H_2O)}$ value of 32 ± 2°. In contrast, 13F forms a moderately hydrophobic ($\theta_{a(H_2O)}$ = 92 ± 2°) SAM (18). Physical adsorption of hFN to glass and EDA-derivatized glass increased the hydrophobicity of the surface such that $\theta_{a(H_2O)}$ = 50 ± 2° and 57 ± 2°, respectively. However, incubation of glass with HS increased the contact angle from 10 ± 2° to 17 ± 2°. HS decreased the contact angle of EDA-modified glass from 32 ± 2° to 24 ± 2°.

EDA and 13F SAMs have been characterized by XPS elsewhere (18). The relative amount of hFN on the surface of the substrate was determined by analysis of the nitrogen content, a function of the N(1s) peak area. The relative nitrogen coverage of EDA/hFN substrates was determined by subtracting the N(1s) peak of the EDA substrates from the N(1s) peak of the EDA/hFN substrate. XPS analysis of EDA and unmodified glass substrates that had been incubated with hFN showed a marked increase in the N(1s) peak on the surface of EDA compared with that of unmodified glass.

Cell Adhesion and Growth. HUVE cells were seen to adhere and spread as early as 4 hr after seeding on EDA and EDA/hFN substrates, whereas few cells adhered to the glass, glass/hFN, and glass/HS before 24 hr. Fig. 1 shows the growth to confluency of HUVE cells initially seeded at 2500 cells per cm^2 on six different substrates after 10 days, as observed by random field observation under differential interference contrast microscopy. EDA and EDA/hFN-modified substrates allowed the fastest rate of growth to confluency under these conditions. In contrast, adsorbed HS inhibited HUVE cell adhesion and growth on both glass and EDA.

bFGF-Dependent Differentiation. bFGF-dependent differentiation of endothelial cells into neovascular cord structures has been described as an angiogenic event (19, 20). HUVE cells that grew to confluency on EDA and EDA/hFN substrates were cultured in growth medium supplemented with bFGF at 5 ng/ml without endothelial cell growth factor, as suggested by Maciag *et al.* (19). After an additional 10–21 days in culture, HUVE cells underwent assembly into preneovascular structures, forming braids of cells and complex multicellular strands (Fig. 2).

Growth on Patterned Substrates. The formation of coplanar EDA/13F SAM patterns using deep UV lithography has been described (15, 18, 21). The resulting patterns are composed of regions containing pure 13F monolayers and EDA monolayers containing 13F at an EDA/13F ratio of 6:1 (18). The surface free energy of EDA films is not significantly affected by this low amount of 13F incorporation ($\theta_{a(H_2O)}$ remains at 35 ± 2°), and the EDA-containing regions exhibit the same degree of adhesiveness for endothelial cells as pure EDA SAMs.

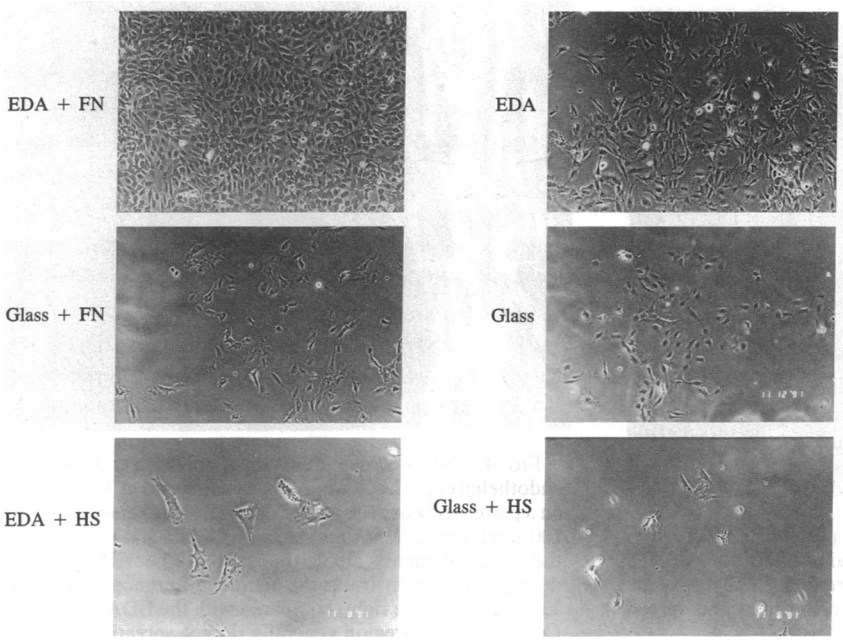

FIG. 1. Growth to confluency of HUVE cells on EDA, EDA/hFN, EDA/HS, glass, glass/hFN, and glass/HS. After 8 days in culture under growth conditions, HUVE cells seeded on EDA/hFN and EDA substrates attain confluency. HUVE cells seeded on HS-modified substrates or unmodified glass were not seen to proliferate or attain confluency.

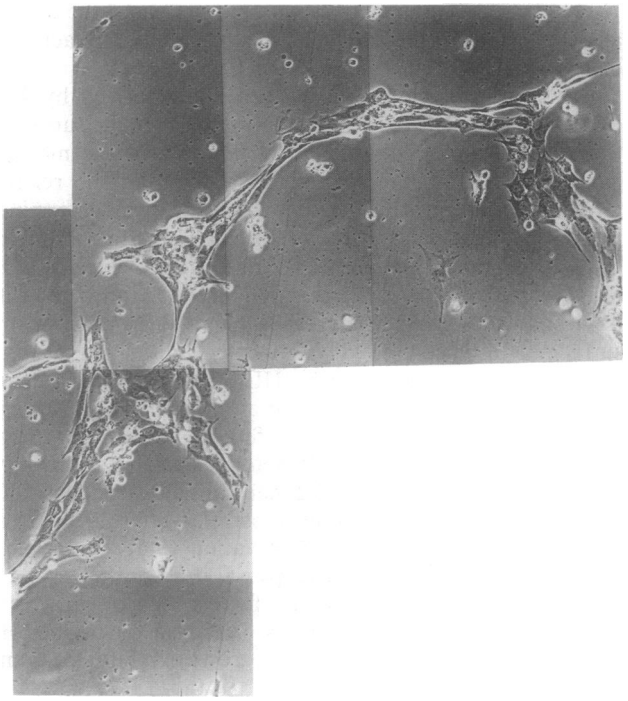

FIG. 2. Endothelial cells grown to confluency on an EDA/hFN substrate. At confluency, medium was supplemented with bFGF at 5 ng/ml. Within 1 week, cells were seen to form neovascular assemblies of tightly packed cells.

Endothelial cells, seeded at 2500 cells per cm^2 on patterns of 100-μm-wide EDA domains against 100-μm-wide domains of 13F, are observed to preferentially attach and elongate in the EDA domains (Fig. 3). Within 4 hr of seeding, the cells at the interface between EDA and 13F are observed to orient and elongate parallel to the EDA/13F molecular interface. The next 12–36 hr showed a rise in the number of endothelial cells that elongate parallel to the EDA/13F interface with increased cell density medial to the interface (Fig. 4*A*). The occasional endothelial cell found on the 13F surface remains rounded and shows little isotropic orientation of microfilaments (Fig. 4*B*).

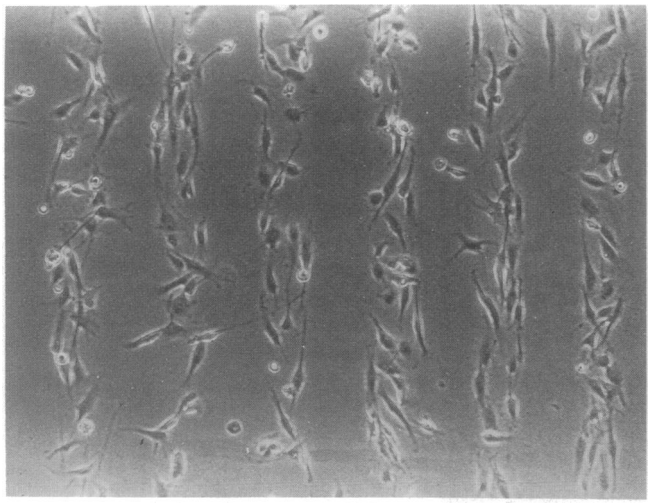

FIG. 3. HUVE cells seeded on substrates previously modified to have distinct 100-μm-wide alternating domains of EDA and 13F. Forty-eight hours after seeding, cells preferentially adhere to the EDA domains; over time these cells are seen to orient and spread parallel to the EDA/13F interface.

Further examination of the role of line-width in the orientation of endothelial cells indicated that the higher the aspect ratio of the lines, the more ordered the cells. In these experiments, endothelial cells were seeded on a coplanar SAM of EDA and 13F with line-widths that varied from 100 to 500 μm. Fig. 5 shows actin-stained endothelial cells 24 hr after seeding on 100-, 200-, and 500-μm line-widths. These fluorescence photomicrographs show a decrease in microfilament ordering with an increase in the line-width. There was no observed difference in the quality of growth and spreading between porcine cerebral microvascular- and human umbilical vein-derived endothelial cells on the EDA surface.

Neovascular Cord Formation. Controlled, defined formation of neovascular assemblies on a two-dimensional coplanar SAM surface is shown in Fig. 6. Endothelial cells were first grown to confluency on EDA lines bound by domains of 13F. After growth and alignment of endothelial cells within the EDA region (demonstrated in Fig. 5), neovascular assemblies were observed to form on the EDA line and aligned with the long axis of the line.

DISCUSSION

Endothelial Cell Adherence and the Cell Cytoskeleton. The formation of neovascular assemblies on EDA lines is a critical point in demonstrating the use of chemical modification of two-dimensional surfaces. In these studies we demonstrated that neovascular assemblies can be formed not only

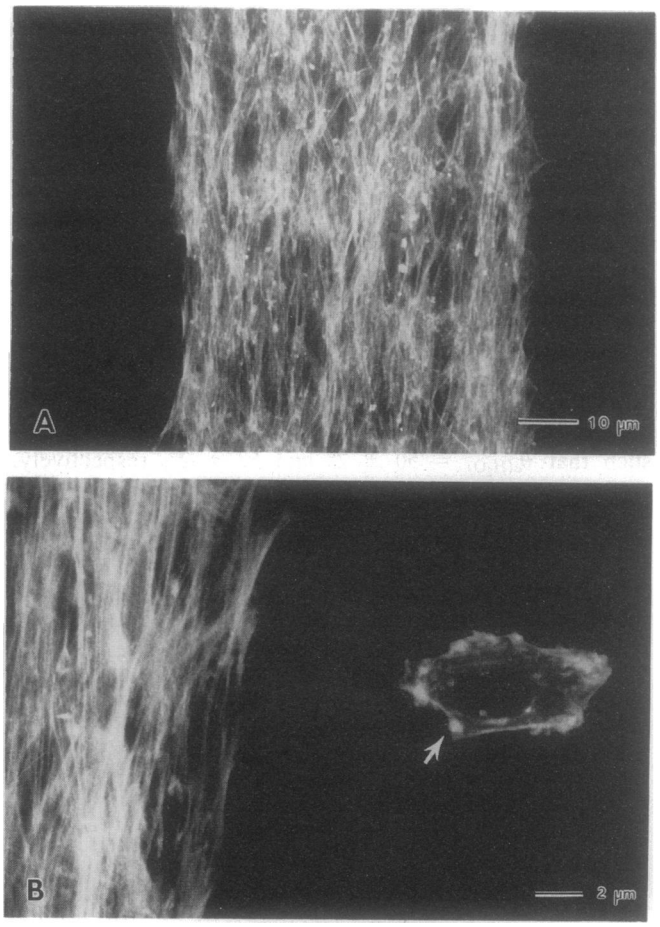

FIG. 4. NBD-phallacidin-stained porcine cerebral microvascular endothelial cells. (*A*) Endothelial cells seeded at 3 × 105 cells per cm^2 on a patterned glass substrate. The pattern is generated by alternating 100-μm bands of EDA and 13F. Phalloidin stain shows alignment of the actin filaments along the axis of the EDA band. (*B*) This micrograph demonstrates the distinct difference in cells found in the 13F region (on the right) compared with the EDA region (on the left). Cells in the 13F region generally do not spread or orient (arrow).

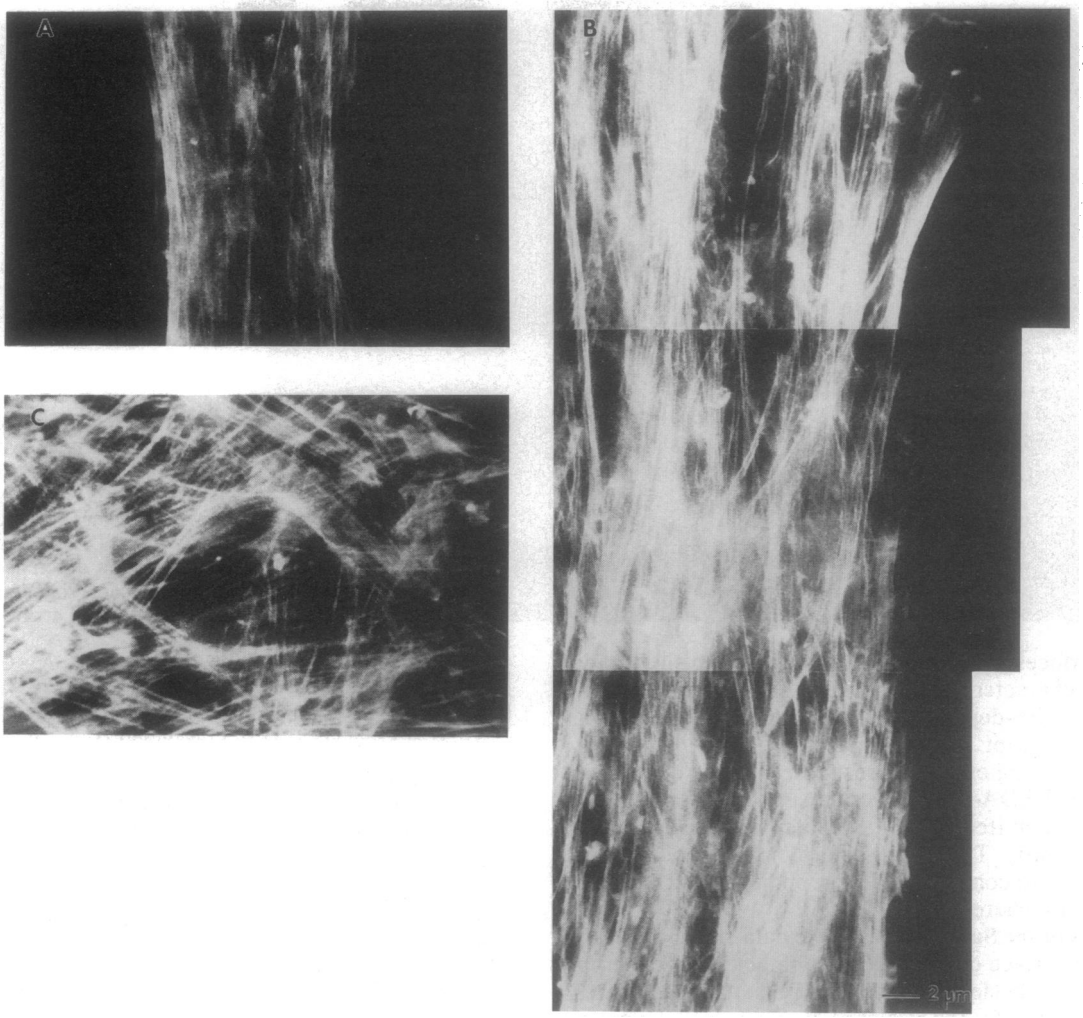

FIG. 5. Porcine cerebral microvascular endothelial cells seeded on a two-dimensional coplanar EDA/13F SAM with 100- (*A*), 200- (*B*), and 500- (*C*) μm-wide bands of EDA. The cells were stained with NBD-phallacidin and show the orientation of actin filaments in the cytoskeleton. Note the highly organized directional cytoskeleton of the cells in the 100-μm line compared with the less organized cytoskeleton of cells in the 200- and 500-μm lines.

on homogenous surfaces of EDA but, importantly, can be restricted to high-resolution EDA regions when bounded by nonadhesive domains (13F).

Endothelial cells preferentially adhered to, elongated on, and proliferated within EDA domains bounded by the 13F regions. Additionally, as the endothelial cells increased in number, there was an increase in the orientation of the cells along the long axis of the EDA/13F interface. The orientation was reflected in the predominant axis of the microfilaments and suggests that the boundary properties of the patterned substrate dictate the initial adherence of the endothelial cells and ultimately the alignment of the cells not only at the EDA/13F interface but many cells distal to the EDA/13F interface.

Varying the EDA line-width demonstrated an aspect ratio-limiting effect, where narrow lines (100 μm) forced the alignment of the cell axis in the direction of the line. Wider line-widths (200 and 500 μm) showed a decrease in the average ordering of the cell axis, and at 500 μm little orientation with the EDA line was retained.

Endothelial cell adherence to EDA appears to be mediated by bound fibronectin, either physically adsorbed before cell seeding or physically adsorbed from the culture serum. This result accords with the observations of others, who have addressed the role of the substratum. Maciag *et al.* (19) used endothelial cells grown on a glass substratum exposed to different concentrations of fibronectin to suggest an optimum level of fibronectin for cellular self-assembly. This effect appeared to depend on the surface character that promotes cell adhesion, where too little or too much fibronectin reduced the ability of a confluent monolayer of endothelial cells to undergo bFGF-dependent differentiation. Hubbell and coworkers (12–14), using endothelial cell-specific binding domains of fibronectin (Arg-Glu-Asp-Val; REDV) immobilized to a nonadhesive substrate, have shown selective adherence and spreading of endothelial cells that remain nonthrombogenic. This result suggests that coplanar substrates with areas rich in REDV or RGD-related peptides would likely promote preferential adherence of cell types with the appropriate cell-surface ligand.

In contrast to the hFN results, the HS-coated surfaces did not promote endothelial cell adhesion, suggesting that specific interactions are more important than the hydrophobicity (24° for EDA-HS compared with 32° for EDA). Charge repulsion between the EDA-HS surface and the high amounts of HS and chondroitin sulfate on the endothelial cell surface (22, 23) might account for this observation. Other cell types with different plasma membrane characteristics may be expected to respond differently. For example, the addition of HS on an EDA surface enhances neuron growth and survival (D.A.S., unpublished data; ref. 24).

Differentiation of Endothelial Cells on Surfaces. Differentiation of endothelial cell monolayers depends on the milieu

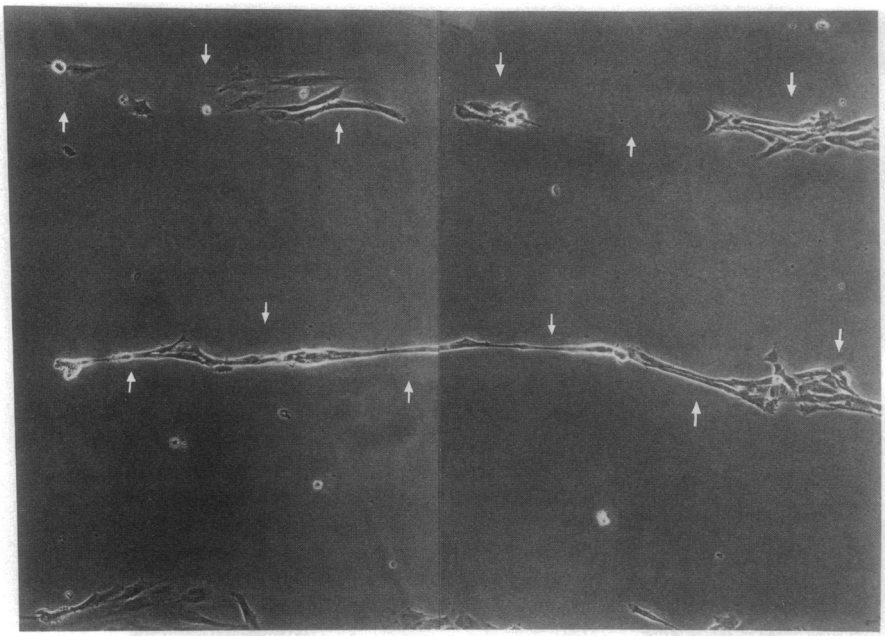

FIG. 6. Neovascular cord formation on a two-dimensional coplanar EDA/13F SAM. The linewidth of EDA is 100 μm with 100-μm-wide 13F lines separating EDA regions. The EDA/13F interface is seen as a slight difference in contrast of the background and is demarcated by small arrows.

and the surfaces. We did not try to distinguish between substratum character and the ability of the endothelial cells to undergo bFGF-dependent differentiation into preneovascular cords, except to note that confluency *in vitro* is a prerequisite for the effect. Under these substrata conditions only EDA and EDA-hFN substrata support growth to confluency and permitted bFGF-dependent differentiation into neovascular cords. The neovascular cords formed on these two substrata are comparable in morphology to neovascular cords seen elsewhere (17, 19, 25, 26).

Properties of the Substratum. These data suggest that it is not only the surface character (hydrophilicity and chemical) that promotes adhesion of endothelial cells. Although there is no direct evidence for the role of hFN as extracellular matrix molecules for the cell-surface-mediated binding of endothelial cells on these substrates, the RDG-binding domains of fibronectin are probably a prerequisite for the initial adhesion of these cells. Ingber and Folkman (27) have demonstrated that fibronectin or other extracellular matrix components (i.e., type IV collagen) are required for endothelial cell attachment and ultimately control the ability of endothelial cells to form tubular networks. Furthermore, one can speculate that serum fibronectin from the medium adsorbs to both the EDA and 13F domains on the glass substrate but that the nature of 13F results in conformational changes in fibronectin that prevent exposure of the RGD-binding domain from being presented (26).

Future Possibilities and Conclusion. These results offer the possibility that directionally controlled neovascularization can be promoted on substrates with chemically modified adjacent adherent and nonadherent domains. Ultimately, these types of chemical modifications may be used to promote and control endothelial cell adhesion and differentiation on the surface of implanted materials such as Gore-Tex and Dacron used in by-pass surgery as artificial vessels and silicones, metals, and ceramics used as mechanical devices.

We are grateful for the technical assistance of Mr. Geoff Stilwell and Ms. Alexandra McPherron for the initial coplanar experiments. We also acknowledge the support of the Naval Research Laboratory through CORE funding of this project to A.S.R.

1. Folkman, J. & Shing, Y. (1992) *J. Biol. Chem.* **267**, 10931–10934.
2. Klagsbrun, M. & D'Amore, P. A. (1991) *Annu. Rev. Physiol.* **53**, 217–239.
3. Montesano, R., Vassalli, J.-D., Baird, A., Guillemin, R. & Orci, L. (1986) *Proc. Natl. Acad. Sci. USA* **83**, 7297–7301.
4. Sato, N., Nariuchi, H., Tsuruoka, N., Nishihara, T., Beitz, J. G., Calabresi, P. & Frackelton, A. R., Jr. (1990) *J. Invest. Dermatol.* **95**, 85S–89S.
5. Sutton, A. B., Canfield, A. E., Schor, S. L., Grant, M. E. & Schor, A. M. (1991) *J. Cell Sci.* **99**, 777–787.
6. Yeager, A. & Callow, A. D. (1988) *Trans. Soc. Artif. Intern. Organs* **34**, 88–94.
7. Form, D. M., Pratt, B. M. & Madri, J. A. (1986) *Lab. Invest.* **55**, 521.
8. Carter, S. B. (1965) *Nature (London)* **208**, 1183.
9. Carter, S. B. (1967) *Exp. Cell. Res.* **48**, 189.
10. Harris, A. (1973) *Exp. Cell Res.* **77**, 285–297.
11. Kleinfeld, D., Kahler, K. H. & Hockberger, P. E. (1988) *J. Neurosci.* **8**, 4098–4120.
12. Hubbell, J. A., Massia, S. P., Desai, N. P. & Drumheller, P. D. (1991) *BioTechniques* **9**, 568–572.
13. Massia, S. P. & Hubbell, J. A. (1990) *Anal. Biochem.* **187**, 292–301.
14. Massia, S. P. & Hubbell, J. A. (1991) *J. Biomed. Mat. Res.* **25**, 223–242.
15. Dulcey, C. S., Georger, J. H., Jr., Krauthamer, V., Stenger, D. A., Fare, T. L. & Calvert, J. M. (1991) *Science* **252**, 551–554.
16. Zisman, W. (1964) in *Contact Angles, Wettability and Adhesion, Advances in Chemistry*, ed. Fowkes, F. M. (Am. Chem. Soc., Washington, DC), Vol. 43, pp. 1–51.
17. Robinson, D. H., Kang, Y.-H., Deschner, S. H. & Nielsen, T. B. (1990) *In Vitro Dev. Biol.* **26**, 169–180.
18. Stenger, D. A., Georger, J. H., Dulcey, C. S., Hickman, J. J., Rudolph, A. S., Nielsen, T. B., McCort, S. M. & Calvert, J. M. (1992) *J. Am. Chem. Soc.* **114**, 8435–8442.
19. Maciag, T., Kadish, J., Wilkins, L., Stemerman, M. B. & Weinstein, R. (1982) *J. Cell Biol.* **94**, 511–520.
20. Klagsbrun, M. & Shing, Y. (1985) *Proc. Natl. Acad. Sci. USA* **82**, 805–809.
21. Georger, J. H., Stenger, D. A., Rudolph, A. S., Hickman, J. J., Dulcey, C. S. & Fare, T. L. (1992) *Thin Solid Films* **210/211**, 716–719.
22. Lowe-Krentz, L. J. & Joyce, J. G. (1991) *Anal. Biochem.* **193**, 155–163.
23. Castillo, C. J., Coburn, P. & Buonassisi, V. (1987) *Biochem. J.* **246**, 687–693.
24. Cotman, C. W., Cummings, B. J. & Pike, C. (1993) in *Neural Regeneration*, ed. Gorio, A. (Raven, New York), pp. 217–240.
25. Feder, J., Marasa, J. C. & Olander, J. V. (1983) *J. Cell. Physiol.* **116**, 1–6.
26. Lewandowska, K., Balachander, N., Sukenik, C. N. & Culp, L. A. (1989) *J. Cell. Physiol.* **141**, 334–345.
27. Ingber, D. E. & Folkman, J. (1989) *J. Cell. Biol.* **109**, 317–330.